Restructuring the Active Site of Fumarase for the Fumarate to Malate Reaction†

Irwin A. Rose*

Institute for Cancer Research, Fox Chase Cancer Center, 7701 Burholme Avenue, Philadelphia, Pennsylvania 19111

Received May 28, 1997; Revised Manuscript Received July 24, 1997⊗

ABSTRACT: Changes in the active site of fumarase (yeast fumarase II) that occur when fumarate is converted to malate (E·F → E·M) must be reversed for another cycle of reaction to take place. As shown here, recycling of the enzyme includes two proton transfers and one conformational change. These events, together with the M-off step, are variously rate-determining depending on the medium. In very low salt the release of M is limited by the conformational change. Thus, $(V/K_m)_F$ decreases with increased viscosity, shown with glycerol. A variety of simple anions, such as Cl^- at ∼50 mM and F itself at low concentration, activate the dissociation of M. This nonspecific anion effect is the basis for the >4-fold apparent cooperative activation by substrate. The M-off step and the conformational change are independent and random-order events. Thus, even when M-off is made rapid the rate of recycling is inhibited by glycerol, which in 100 mM NaCl inhibits V_{max} but not V/K_m. The enzyme form that results when M is released is M-specific, E_m. Thus mesotartarate, competitive toward M, is noncompetitive toward F. The slow conformational change required for recycling of E_m is activated by P_i and chaotropic anions such as azide and thiocyanate, giving rise to a nonspecific intermediate, E_{mf} (mesotartarate becomes competitive toward F and Britton's countertransport property disappears with these activators). Evidence is presented for the locations and rates of the two proton transfer steps required to complete the cycle.

The class II fumarases (fumarate hydratase: EC 4.2.1.2) are metal ion-independent homotetrameric enzymes of widespread distribution, belonging to a sequence-related family that includes aspartase, adenylosuccinase, and arginosuccinase, all of which produce fumarate by 1,2-elimination. The dehydration of malate (M) by fumarase is believed to occur by the stepwise abstraction of the C-3*R* proton of M followed by removal of C2-OH of an acicarbanion intermediate (Porter & Bright, 1988; Anderson, 1991). These chemical interconversions are the most facile steps of the reaction cycle as indicated by rapid [2-^{18}O]malate/H_2O exchange (Hansen et al., 1969; Berman, 1971) and the absence of a rate difference with [3-^{2}H]malate (Fisher et al., 1955; Hansen et al., 1969). The effects of viscosogens such as glycerol, which decrease *V/K* of both substrates, have been attributed to viscosity-sensitive conformational changes, possibly at the product-off steps (Sweet & Blanchard, 1990).

Two observations indicate the importance of steps subsequent to product release, *exorecycling*,[1] for determination of k_{cat}. First, by applying the countertransport method of Britton (1973), it was shown that during conversion of substrate to product the ratio of a test mixture of labeled reactants, initially at equilibrium, was displaced in the direction counter to that of net mass flow until equilibrium was reached (Rose et al., 1993; Rebholz & Northrop, 1995). Counterflow observed with fumarase at remarkably low concentrations of substrate shows that the interconversion of ligand-free isoforms that have different absolute or relative specificities for F and M is not rapid. Thus, a value K_α^F of ∼0.1 mM characterizes the concentration of fumarate (about 2−3x K_m^F) that will equally partition a fumarate-specific isoform between recycling and reaction with fumarate to form malate or, indistinguishably, a malate-specific isoform between counterflow of malate and recycling.

Second, slow recycling of the abstracted C-3 proton of malate, suggested by equilibrium exchange studies (Hansen et al., 1969), was confirmed by showing intermolecular T transfer using doubly-labeled malate: 3T-malate* + fumarate → 3T-malate + fumarate*. Little more fumarate than its K_m concentration was required for 50% T-capture (Rose et al., 1992). The presence of the C-3-derived proton on the enzyme after dissociation of fumarate might provide a basis for fumarate specificity. However, transfer of this proton cannot be responsible for a slow recycling step given the absence of either a rate effect with [3-^{2}H]malate or discrimination in forming M from F in T-water (I. A. Rose and D. J. Kuo, 1995, unpublished results). Thus, a more complex scheme of recycling must be considered.

As no metal cofactor is required for activity, fumarase II must depend on a proton to promote abstraction of the C2-OH of malate in forming the product water:

$$E^{\alpha H}\cdot M \leftrightarrow E_{\beta H}^{\alpha H_2O}\cdot F \leftrightarrow E_{\beta H}^{\alpha}\cdot F + H_2O$$

[From the exchange data of Boyer's group (Hansen et al., 1969; Berman et al., 1971), H_2O is released before F.] The

† This work was supported by NIH Grants GM20940 to I.A.R. and CA06927 (to the Institute for Cancer Research) and by an appropriation from the Commonwealth of Pennsylvania.

* Address correspondence to this author c/o Dr. Ralph Bradshaw, Department of Physiology and Biophysics, University of California at Irvine, Irvine, CA 92717. Tel: (714) 824-6236. FAX: (714) 824-8036.

⊗ Abstract published in *Advance ACS Abstracts,* September 15, 1997.

[1] The term "exorecycling" refers to the segment of the reaction cycle *after* product release and *before* interaction of free enzyme with substrate. Isomechanism kinetics are observed when *exo* events contribute significantly to k_{cat}. All other steps *except* those involved in the reaction chemistry are referred to as *endo*. Endo events are usually lumped with rate constants for product release in steady-state equations. Product release and substrate binding are also defined as endo steps. The last phase of the reaction cycle, the chemical interconversion(s), is usually referred to as the central phase. Net changes that occur between central complexes must be reversed in endo and/or exo steps of the cycle in order for an enzyme to act as a catalyst.

S0006-2960(97)01258-0 CCC: $14.00

step in which this proton is recovered from solvent by the α subsite after the F is produced could be the origin of the observed slow recycling. Of course, if the E·M ⇔ E·F interconversion results in a conformational change the remainder of the reaction cycle must include steps in which the change is reversed. Conformational restructuring may occur during product liberation, commonly spoken of as "induced fit" in the reverse, or after product release and independent of substrate in an isoform fluctuation model. Likewise, proton transfers may occur prior to or during product formation, endorecycling, or after product release.

Aims of the studies described in the present paper are to determine the site at which slow recycling events take place in the fumarase cycle and to clarify the basis for isoform specificity and interconversion. The approaches taken should be useful with most enzymes. Demonstration of noncompetitive inhibition by a product analog can provide important evidence for an isomechanism (Rebholz & Northrop, 1994, 1995) and establish both the existence and the substrate specificity of a slowly recycling free enzyme intermediate. The magnitude of the intercept inhibition constant, K_{ii}, will inversely reflect the concentration of the intermediate with which the inhibitor interacts. A factor that increases recycling will decrease the concentration of the intermediate and result in an increase in K_{ii} if the step that is activated is downstream of the intermediate. Factors that act subsequent to product release should not alter the slopes of double-reciprocal plots or the rate of M/F isotope exchange at equilibrium unless they act after substrate addition in the next cycle. The pH dependence and D_2O effects on K_{ii} may indicate the participation of recycling protons in the composition of an intermediate. The present study makes use of these methods to identify recycling steps in the F → M direction. A subsequent paper will analyze the major recycling pathway of the reverse reaction.

To aid the reader, a summary of the proposed steps of the F → M recycle is shown in Scheme 1.

Scheme 1

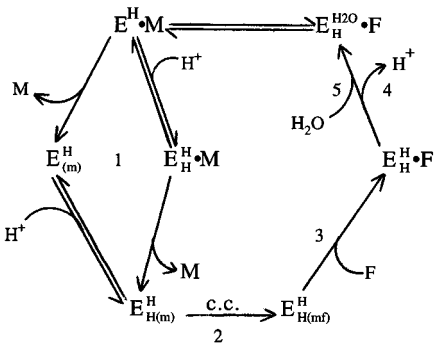

In summary, the chemical step imposes at least one conformational change and two proton transfers that must be reversed either before or after dissociation of M for the next reaction with F to occur. Begin with E^H·M, where H of the α site is derived from the H_2O used for hydroxylation of F. M-dissociation, made rapid by almost any monoanion, produces either $E^H_{(m)}$ or $E^H_{H(m)}$, both of which are M-specific. Rapid equilibration of the β site with protons of the solvent occurs before or after M is liberated, step(s) 1, with a pK_a 6.7. While unfavorable above pH 7, the two-proton state can be promoted in a complex with imidazolium ion, general acid catalysis. A conformational change (c.c.) occurs in the conversion of the M-specific isoform to a nonspecific species $E^H_{H(mf)}$ without change in protonation, step 2. Step 2 is activated by P_i and chaotropic anions. Following reaction with F (step 3), loss of the α-proton occurs (step 4), replaced by an H_2O (step 5). This scheme accounts for all the kinetic and isotopic observations. This is not to suggest that it is unique in doing so, of course.

EXPERIMENTAL PROCEDURES

Protocols: The Britton Counterflow Experiment. In one of two procedures, a standard probe solution of ^{14}C-labeled substrates with high specific activity is brought to equilibrium enzymatically in a microcuvette. Identical amounts of this stock are added to cuvettes containing additional enzyme followed by fumarate. Reaction progress is stopped with acid at fractions, *f*, of progress toward equilibrium, $(M/F)_{eq} \sim 4.4$, and samples are analyzed for total radioactivity in fumarate. K_α is calculated according to a form of the Britton equation (Britton 1973)

$$(F^*/F^*_{eq}) - 1 = K_{eq}(1 - f)[1 - (1 - f)^{F_\infty/K_\alpha}] \quad (1)$$

where $F_\infty = [F]_{eq}$ and K_α corresponds to the concentration of substrate required to capture half of a partitioning species as in the usual substrate partition experiment (Rose et al., 1974), with the exception that K_α is more responsive to the smaller of the two recycling rate constants

$$\vec{k}_{exo}\cdot\overleftarrow{k}_{exo}/(\vec{k}_{exo} + \overleftarrow{k}_{exo}) \equiv \bar{k}_{exo} = k_{cat}\cdot K_\alpha/K_m \quad (2)$$

where $\vec{k}_{exo}$ and $\overleftarrow{k}_{exo}$ represent the rate constants for the interconversion of a pair of isoforms. Thus,

$$\bar{k}_{exo}/k^F_{cat} = K^F_a/K^F_m \quad (3)$$

In a second approach the incubation contains unlabeled substrate and labeled product at zero time. If recycling is rapid, $K^S_\alpha > S_\infty$, or if the free enzymes are not substrate-specific, the appearance of label in substrate will correspond to the progress toward equilibrium, *i.e.* $S^*/S^*_{eq} \cong f$. Appearance of label in excess of this minimum should follow (transposed from Britton, 1973)

$$S^*/S^*_{eq} - f = -(1 - f)(1 + K_{eq})[(1 - f)^{S_\infty/K_\alpha} - 1] \quad (4)$$

An advantage of the P* → S* experiment is that it does not require the prior adjustment of the isotope probe to equilibrium. More importantly, the results at early times can be used to calculate the partition of E_p between its completion of the cycle and counterflow (S → P/P* → S*), where P* → S* is calculated from the average specific activity of the product during the interval of its formation. Changes in the components of this flux ratio make it possible to determine whether effects on K_α are exo or endo derived.

The Equilibrium Exchange Experiment. The rate of isotope exchange at equilibrium includes endo steps only and should not be affected by factors that alter exorecycling. The M/F exchange rate, v_x, is determined using a ^{14}C-trace of M* in an M/F equilibrium. Reaction is initiated with $\sim 5 \times 10^{-6}$ μmol of enzyme/mL and samples were removed for determination of F* at zero time, at two time points, and at equilibrium. Rates agreed closely when calculated from *f*, the fraction of F* toward isotopic equilibrium, and time, *t*, using $v_x t = -([M][F]/[M] + [F])\ln(1 - f)$.

The total radioactivity in fumarate for the above experiments was determined as follows: disodium fumarate (125 μmol) and HCl (300 μmol) were added to each sample, final volume ~0.5 mL. Crystallization of fumaric acid, initiated by vortexing, is rapid at 4 °C. Separated by centrifugation, dissolved in hot water (0.5 mL) and recrystallized (2 or 3 times) to a constant specific activity, the recovery of carrier F was ~50%.

All rates were measured at 25 °C in 1 mL cuvettes following the formation or disappearance of absorbance due to fumarate at 240−280 nm using the ϵ_λ values of Alberty et al. (1954) and the Spectronic 1001 of Milton Roy Co. Linear double-reciprocal plots showing the reciprocal of the initial absorbance change/min are presented and best lines are drawn using a least-squares program.

K_{ii} and K_{is} values were obtained from double-reciprocal plots of rate data + inhibitors:

$$K_{ii} = [\text{inhibitor}]/\left(\frac{\text{intercept}^+}{\text{intercept}^-}\right) - 1 \quad \text{and}$$

$$K_{is} = [\text{inhibitor}]/\left(\frac{\text{slope}^+}{\text{slope}^-}\right) - 1$$

Care was taken in the preparation of all solutions to avoid their contamination with salt derived from the glass electrode used in pH determination. Hence, pH determinations of stock solutions were made on appropriately diluted samples of reagents and on incubation mixtures at the end of each reaction.

Materials. Yeast fumarase was a generous gift of Dr. J. S. Keruchenko of the A. N. Bach Institute of Biochemistry, Moscow, Russia. The enzyme, supplied in 5 mM mesotartarate and 20% ethylene glycol, is perfectly stable in the cold. Many of its physical and kinetic properties have been reported (Keruchenko et al., 1992).

[U-^{14}C]Malate was prepared from [^{14}C]aspartate by incubation with α-ketoglutarate and glutamic−oxalacetic transaminase in combination with NADH and malate dehydrogenase. [U-^{14}C]Fumarate was prepared from [^{14}C]aspartate plus aspartase (prepared from *Escherichia coli*) following absorbance at 240 nm. The reaction was quenched promptly to limit the action of a trace of fumarase. Malate and fumarate were separated on a column of Dowex-1 formate eluted with 2 N formic acid. Formic acid was removed *in vacuo* without heat. Both preparations were made by Donald J. Kuo of this laboratory.

RESULTS

Activation by Low Concentration of Anions. Figure 1 shows the activation of rate resulting with F greater than 0.2 mM. This property, characterized as negative cooperativity, has been reported with fumarase of yeast (Keruchenko et al., 1992) and pig heart (Alberty et al., 1954), and is found with fumarase C of *E. coli* (I. A. Rose, unpublished results). This phenomenon is lost when 100 mM NaCl is included in the F → M direction. At low F, an ~4-fold activation by NaCl is seen. All anions tested were effective (with the millimolar concentration giving half the maximum activation): ClO_4^- (4), SO_4^{2-} (4), BF_4^- (7), formate$^-$ (16), Cl^- (50), acetate$^-$ (50), glycolate$^-$ (50), and P_i (<5). As shown in Figure 1 (inset), MOPS itself activates very well. Although there are previous reports that P_i caused activation with loss of cooperativity (Alberty et al., 1954; Keruchenko et al., 1992), the range of ions able to do the same, many of them without the complication of competitive inhibition found with P_i, has not been appreciated.

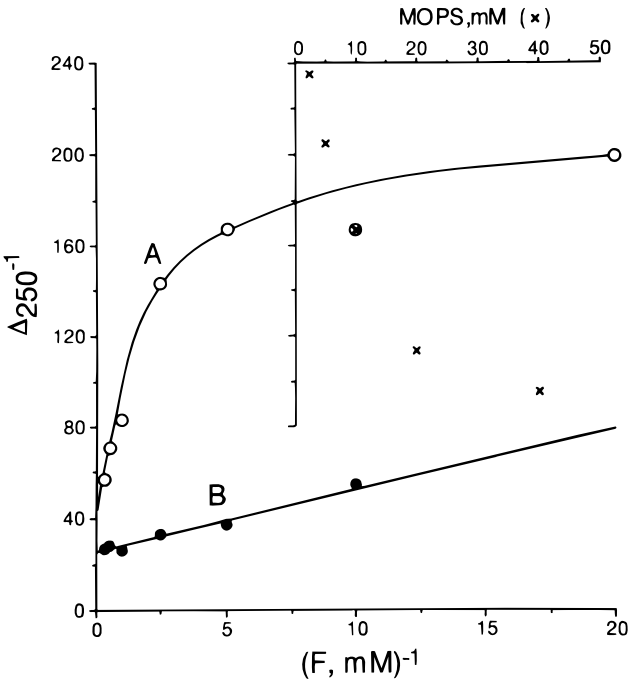

FIGURE 1: Activation of F → M by NaCl and MOPS. Curves A and B show reciprocal rates (Δ_{250}/min)$^{-1}$) *vs* reciprocal F concentration in 10 mM MOPS, pH 7.48, with 100 mM NaCl in curve B. The inset shows the reciprocal rates, same scale, at 0.1 mM F and varying MOPS without NaCl. From curve B and the enzyme concentration, $k_{cat} = 165$ s^{-1}, $K_m^F = 0.12$ mM.

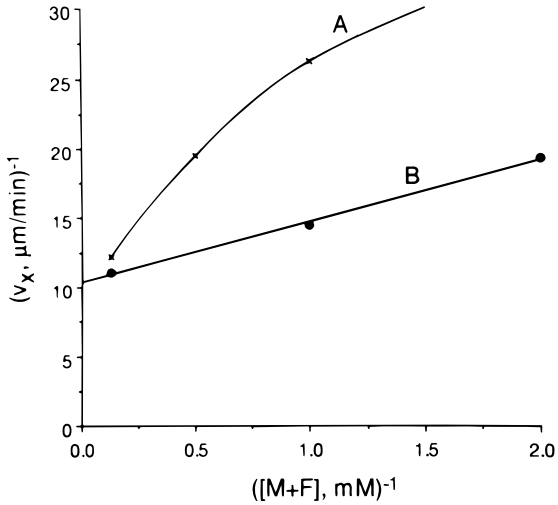

FIGURE 2: M/F equilibrium exchange rate is cooperative and activated by NaCl. Reciprocal plots: [M + F] at equilibrium from 0.5 to 8 mM, in 20 mM MOPS, pH 7.5, with NaCl (100 mM) in curve B only. $V_x = 140$ s^{-1}.

The effects of simple monoanions at the concentrations indicated reflect activation of free M production and not activation of exorecycling. Thus, a biphasic double-reciprocal relationship observed on the M/F equilibrium exchange rates *vs* substrate concentration is linearized by Cl^- with activation (Figure 2). Since equilibrium exchange rates do not include exorecycling steps and the reaction chemistry is rapid, the activation and loss of cooperativity due to Cl^- must occur at or before product release.

Figure 3 compares the effects of Cl^- concentration on initial rate, F → M at 0.5 mM F, and on K_α, the parameter

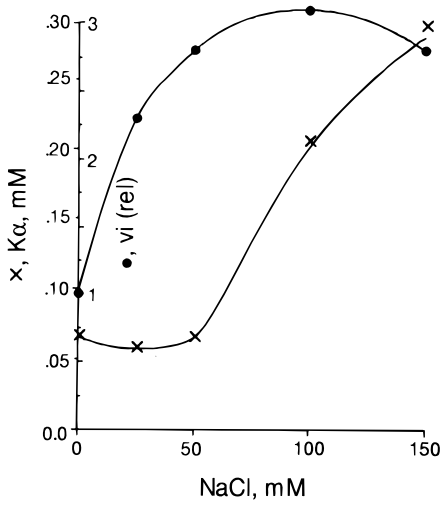

FIGURE 3: Effect of [NaCl] on initial rate and countertransport. An M*/F* equilibrium probe is added to 0.5 mM F, 25 mM Hepes, pH 7.5, and varying NaCl concentrations (0−150 mM). Values of K_α (×) were calculated from F* determined at $f = 0.5$ using eq 1. For extent of activation (●), v_i(rel), use the right ordinate axis.

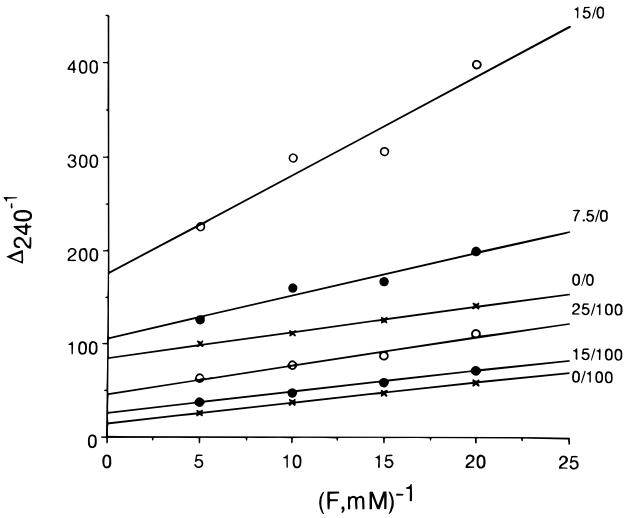

FIGURE 4: Effect of glycerol on $(V/K_m)_F$ in the presence and absence of NaCl. With 10 mM MOPS, pH 7.4, the designation 25/100 represents (25% of glycerol by volume)/(100 mM NaCl), *etc.*

sensitive to the recycling/counterflow ratio. Little net change in K_α is seen up to 50 mM Cl^-, where activation of initial rate is half-maximal. The increase in K_α to 0.2 mM at 100 mM NaCl will be shown below to be due to the activation of exorecycling by some anions at high concentration.

The inhibitory effect of viscosogens attributed to a slow conformational change, reported with heart enzyme by Sweet and Blanchard (1990), is also seen with yeast fumarase in the absence of NaCl (Figure 4). Significantly, the large effect on $(V/K_m)_F$, 3.6-fold caused by 15% glycerol, which indicates a conformational change at or prior to the product release step, is not seen in the presence of NaCl. On the other hand, a 2.75-fold inhibition of V_{max} by higher glycerol (25%) only caused a 1.4-fold decrease on V/K_m in NaCl, suggestive of a slow conformational change subsequent to release of M. A simple interpretation of the independent effects of salt and glycerol is that they influence different steps in the reaction cycle.

Origin of Activation by Substrate. The nonspecificity with respect to activating anion and the fact that both Cl^- and high substrate activate equilibrium exchange suggest that

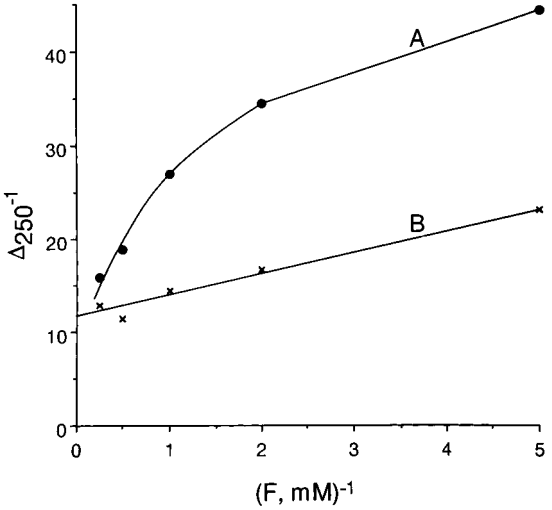

FIGURE 5: Activation by F is only an anion effect. As in Figure 1, except curve B has 4 mM disodium malonate, pH 7.39, instead of NaCl.

activation by F may result from its action as an anion and not as substrate. This would be supported if nonsubstrate dicarboxylic acids activated as well as F, at much lower concentrations than does acetate. Malonate and acetate were found to give about the same ultimate, 3-fold activation with K_A of 2 and 25 mM, respectively (not shown). The activation by fumarate, seen above 0.5 mM, occurs with 4 mM malonate and F at <0.2 mM (Figure 5). Activation by F is about 50% complete at 1−2 mM F (Figures 1 and 5), which is approximately the K_A found for malonate. Since *all* negative cooperativity is abolished with sufficient Cl^- or malonate, it can be concluded that cooperativity caused by F is due entirely to its effect as an anion facilitating the liberation of M.

E_m, an M-Specific Enzyme Isoform. Mixed noncompetitive inhibition is shown by mesotartarate using F as substrate in 100 mM NaCl: $K_{ii} \sim 2.6$ mM and $K_{is} \sim 1.9$ mM at pH 7.48 (Figure 6). With M as substrate, mesotartarate is seen to be competitive, $K_{is} \sim 1$ mM. High M, 10−30 mM, was required to obtain linear extrapolations in this region of substrate activation. An M-specific isoform, designated E_m, must be present in the reaction cycle with F as substrate. Similar inhibition patterns were shown with 1,2,4,5-benzenetetracarboxylic acid (or pyromellitic acid), $K_{ii} \sim 100$ μM and $K_{is} = 10$ μM; with citrate, $K_{ii} \sim 20$ mM and $K_{is} = 3$ mM; and with *trans*-aconitate, $K_{ii} = 2.4$ mM and $K_{is} = 0.14$ mM, all measured at pH 7.4. Unlike mesotartarate, where $K_{is}/K_{ii} \sim 1$, the slopes are much more sensitive than intercepts with these three inhibitors. This difference in relative affinities suggests that additional isoforms with different relative affinities may be present in the reaction cycle.

Ionic Effects on Recycling. As noted in Figure 3, high NaCl causes an increase in K_α. This suggestion of faster recycling was tested by determining the effect of NaCl and other salts on the noncompetitive inhibition constant, K_{ii}, of mesotartarate. An increase in K_{ii} value would imply a lowered steady-state concentration of E_m. This interpretation could be complicated if at high concentration the tested anion was noncompetitive itself. Figure 7 shows that K_{ii} of mesotartarate is increased 1.7-, 2.2-, and 5.4-fold by NaN_3 at 5, 10, and 20 mM, respectively, all in 100 mM NaCl. Activation by N_3^- occurs with no change in slope, indicating

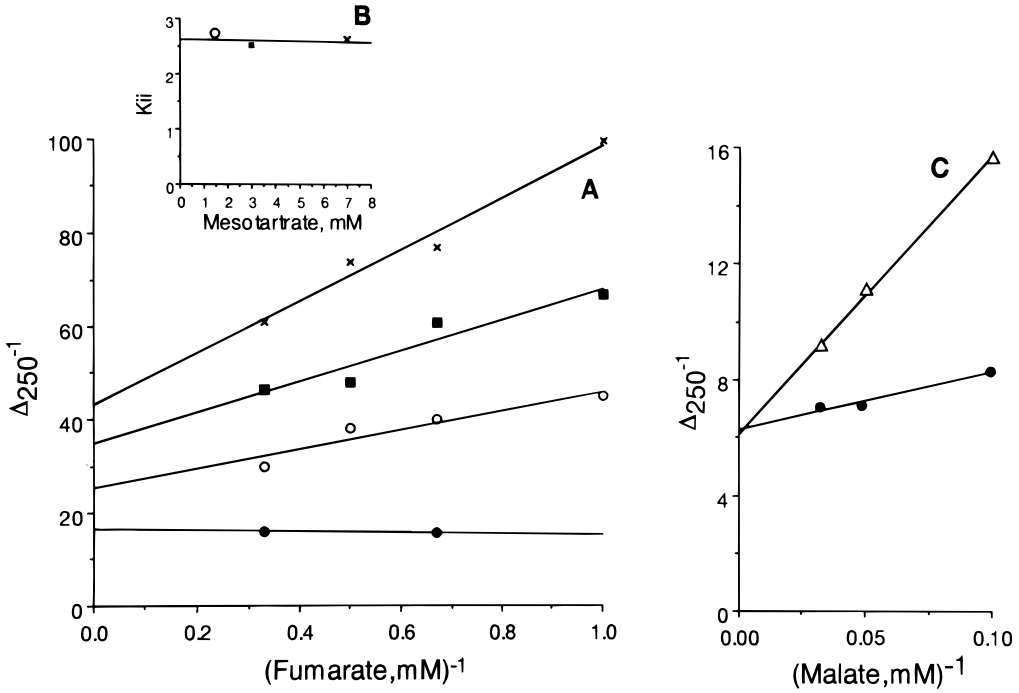

FIGURE 6: Mesotartarate, a malate analog that is noncompetitive *vs* F. (A) Double-reciprocal plot with F ± mesotartarate. As in Figure 1B (●) or with mesotartarate (1.5 mM, ○; 3 mM, ■; and 7.0 mM, ×). (B) K_{ii}(mesotartarate) *vs* [mesotartarate], calculated using A. (C) Reciprocal plot with M ± mesotartarate, ● or Δ (4 mM).

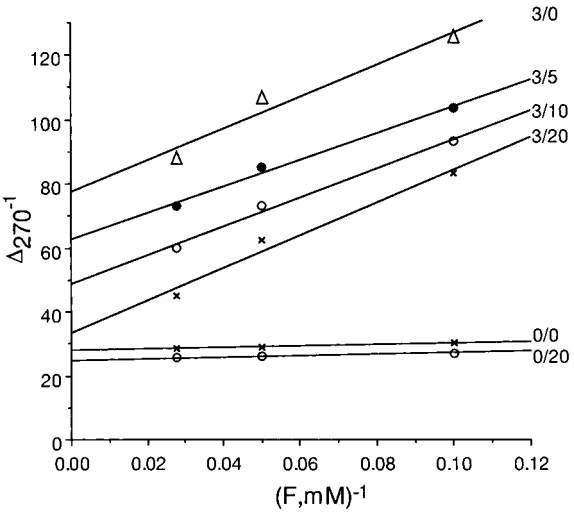

FIGURE 7: Azide decreases the intercept effect of mesotartarate. Like Figure 1B with the noted mesotartarate/NaN_3 combinations (both millimolar).

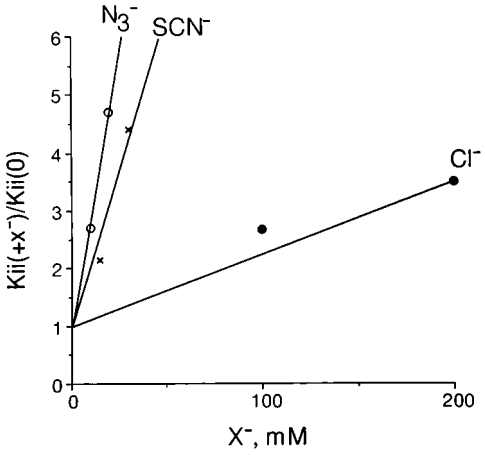

FIGURE 8: Comparison of the effect of N_3^-, SCN^-, and Cl^- on K_{ii} of mesotartarate. The K_{ii}s of mesotartarate at 3 mM were determined at pH 7.4 (10 mM MOPS) in the presence of 100 mM NaCl and the noted added salt NaX (millimolar). The ordinate gives K_{ii} relative to the values obtained with no additional salt, only the 100 mM NaCl common to all.

that activation is subsequent to product release and that azide is not a competitive inhibitor in this range. At 100 mM NaN_3 (not shown), mesotartarate, at 3 mM, acts like a competitive inhibitor; *i.e.*, its K_{ii} has been increased more than 10-fold. No noncompetitive effect of azide was evident at this concentration either. Figure 8 compares NaN_3, NaSCN, and NaCl for their ability to increase K_{ii} of mesotartarate, presumably by increasing the recycling of E_m. The greater effect shown with the chaotropic anions does not extend to cations and therefore is probably not due to an effect on solvent (Collins, 1997). Thus, the K_{ii} values of mesotartarate with chaotropic cations Cs^+ and guanidinium$^+$ were no different than with nonchaotropic Na^+, compared as their chlorides at 200 and 300 mM.

Buffer Effects on Recycling. Imidazole activates initial rate and raises K_{ii} of mesotartarate in the F → M direction. At pH 7.4 the maximum rate was increased 1.7-fold by 50 mM imidazole (Figure 9) with no further increase with 100 mM. A 4.4-fold increase in K_{ii} is observed in the limit of high imidazole, also suggesting a saturation phenomenon. The absence of a change in slopes indicates that both rate and K_{ii} effects are due to increased recycling of E_m. In support of this, imidazole increases K_α (shown below) and has almost no effect on M/F equilibrium exchange rate (not shown). To determine whether the acid or base component of imidazole causes the activation, the effects of two buffers with different p*K*s were compared. Imidazole (pK_a 6.9) was 7.9× more effective at pH 7.4 than 2-ethylimidazole (pK_a 8.0) (Figure 10). This ratio is much closer to the prediction for general acid catalysis, 3.6, than for general base catalysis, 0.31. In the limit, the same maximum activation is found for both buffers, 2.4×. In spite of what appears to be a buffer effect on K_{ii} of mesotartarate, there was no effect of D_2O on

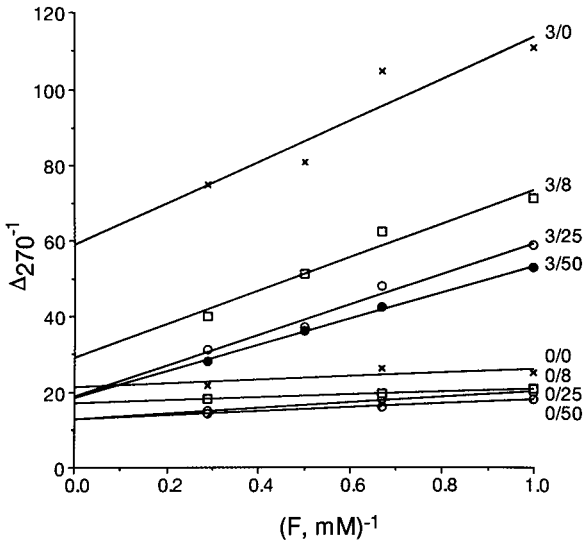

FIGURE 9: Effect of imidazole on K_{ii} of mesotartarate. Incubations contained MOPS (10 mM, final pH 7.30−7.48) and mesotartarate/imidazole combinations as noted (both millimolar). The Cl^- added with the imidazole was supplemented with NaCl to give 100 mM Cl^- in each incubation. K_{ii} values at 0, 8, 25, and 50 mM imidazole are 1.78, 2.5, 7.0, and 7.8 mM, respectively.

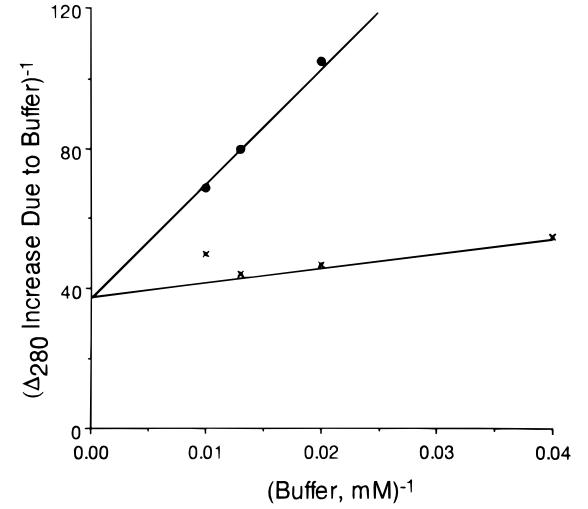

FIGURE 10: Is imidazole an acid or base buffer? Incubations contained 10 mM MOPS, final pH 7.40, and imidazole (×) or 2-ethylimidazole (●) as their chloride salts as noted with total Cl^- adjusted to 100 mM with NaCl in each case. F = 8 mM. The rate in each case was compared to the rate without buffer to determine the increment due to buffer.

K_{ii}; *i.e.*, effects of D_2O on V_{max} were the same in the presence or absence of inhibitor.

Activation by P_i and Alkyl Phosphonates. As reported earlier (Rose et al., 1993) P_i at 10 mM is able to eliminate counterflow observed with either M and F as substrate. Similar results are obtained with yeast fumarase with low concentrations of methyl and propyl phosphonates. These are much less inhibitory than P_i at low concentration of substrates. Making use of their different pK values, these alkyl phosphonates can be compared as activators to determine whether they act as buffers. The K_{ii} values of mesotartarate (using F) are increased by the phosphonates with no effect on slope. For example, see Figure 11, in which 1 mM of either phosphonate increased k_{cat} significantly and increased K_{ii} of mesotartarate ~2-fold. The two phosphonates were about equally effective, both increasing K_{ii} ~2-fold at 1 mM, whether the pH was 7.07, 7.34, or 8.2 although they differ in pK_a by 1 unit (7.1 and 8.18 for methyl and propyl, respectively). These results are not consistent with action of phosphonate as a buffer, nor is it possible to attribute their effect exclusively to either the mono- or dianion forms. Apparently, the two charged species are indistinguishable as activators; *i.e.*, a single charge is sufficient for activation. Consistent with the large effect that 10 mM P_i had on recycling with heart fumarase (Rose et al., 1993), mesotartarate loses its noncompetitive characteristic in the presence of 5 mM methyl phosphonate without change in slope. With what form of the enzyme is mesotartarate interacting competitively with respect to F when E_m has been reduced to nil? To explain the constant slope, one must postulate interaction of the phosphonate with a nonspecific isoform, hence E_{mf}.

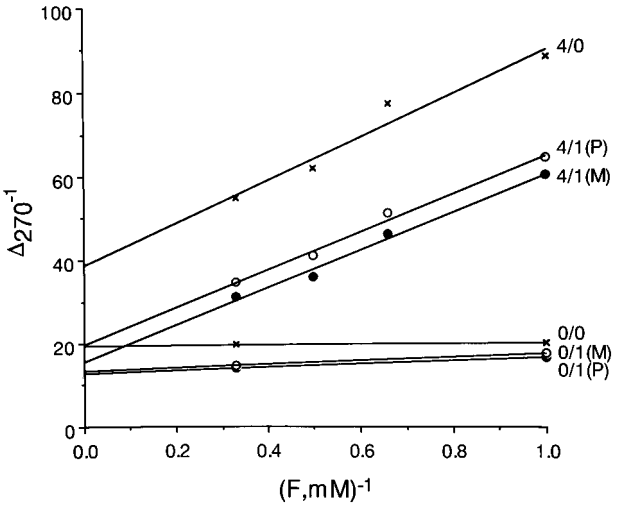

FIGURE 11: Alkyl phosphonates activate and raise K_{ii} of mesotartarate. Incubations contained 10 mM MOPS, pH 7.07, 100 mM NaCl and the noted additions: (mesotartarate)/methyl (M) or propyl (P) phosphonate (both millimolar).

Table 1: Effects of Glycerol, CH_3-PO_3, N_3^-, and Imidazole on K_α in 100 mM NaCl

added[a]	initial rate (rel)	$(F^*_{0.5}/F^*_1) - 0.5$	K_α (mM)	K_α/K_m
0	1	1.56	0.29	2.2
Glycerol (20%)	0.57	2.57	0.08	0.89
CH_3-PO_3 (5 mM)	1.62	0.16	4.0	25
NaN_3 (30 mM)	1.43	0.50	1.2	3.2
Imidazole (40 mM)	1.36	0.20	3.2	10

[a] Each incubation contained MOPS (10 mM, pH 7.35), NaCl (100 mM), F (2 mM), M* (~4×10^4 cpm/mL), and enzyme. Samples were taken at $f = 0$, 0.5, and 1 for determination of F*. Initial rates, as Δ_{260}, are compared and K_α determined from $(F^*_{0.5}/F^*_1) - 0.5$ using eq 4.K_m^F values were determined for each reaction condition for calculation of K_α/K_m.

In the presence of 100 mM NaCl used to activate the dissociation of M, glycerol, chaotropic anions such as N_3^-, imidazole buffers and phosphoanions have been shown to affect V_{max} and not $(V/K_m)_F$ (Figures 4, 7, 9, and 11). The inference that these factors act on a slow exorecycling step was tested by determining their effect on the ability of F to induce the counterflow of M*. Factors that increase recycling should decrease counterflow, $(F^*_f/F^*_i) - f \rightarrow 0$). Those that decrease recycling should increase (F^*_f/F^*_i) relative to the control. Table 1 shows 4−13-fold increases in K_α for the three activators, and the expected decrease for inhibitory glycerol. Using eq 3, the degree to which $\bar{k}_{exo}$ limits k_{cat} (full control implied when K_α/K_m ~1) is shown in the order with glycerol > no addition > with N_3^- and

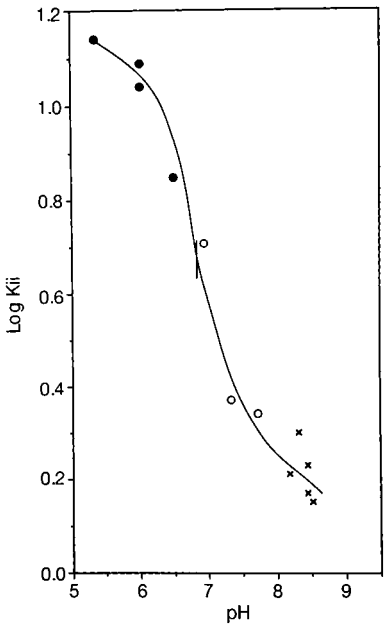

FIGURE 12: pH dependence of K_{ii}(mesotartarate). Reciprocal (F) vs rate curves were plotted ± mesotartarate, as in Figure 6. pH was adjusted with 10 or 20 mM cacodylate (●), MOPS (○), or EPPS (×).

minimally with imidazole and phosphonate at their test concentrations.

Effect of pH on K_{ii} of Mesotartarate. The absence of a D_2O effect on K_{ii} suggests that the rate-limiting utilization of E_m may be *preceded* by a rapid protonation and that $E_m \rightarrow E_{mf}$ itself is not dependent on proton transfer. This would be consistent with the activation of these steps by azide (and high Cl^-), neither of which is a proton donor at pH 7.4. It was of interest to test the pH dependence of K_{ii} of mesotartarate on the possibility that the state of protonation of E_m might affect its affinity for mesotartarate. One could hope in this way to identify the pK_a of the group involved in rapid exorecycling protonation in the F → M direction. An ∼6-fold increase in K_{ii} is found from pH 7.4−8.4 of ∼2 mM to pH 5.3−6.0 of 12 mM (Figure 12). From reciprocal plots (not shown) with mesotartarate present at 3 mM there was little change in slope between pH 6 and 8, consistent with the exo position of the pH effect. At the midpoint of this change, pH ∼ 6.75, only about 1% of the mesotartarate will have been titrated based on pK_2 ∼ 4.75 determined in 100 mM NaCl. Apparently, protonation of E_m prior to its conversion to E_{mf} decreases its affinity for mesotartarate but does not prevent formation of an inhibitory complex. A group with a pK ∼ 6.75 may both decrease the affinity of E_m for mesotartarate when protonated and be required to be protonated for the transformation to E_{mf}.

What Is the Rate-Limiting Step in F → M When E_m → Nil? V_{max} of F → M at pH 7.4 and 100 mM NaCl, ∼300 s^{-1}, is increased 1.45−1.5-fold by addition of NaN_3 or phosphonates. This new activated rate is decreased 2.6-fold in D_2O at 8 mM F and 5 mM methyl phosphonate and 2.0-fold with 100 mM NaN_3, both with 100 mM NaCl. To determine whether the step responsible for the D_2O effect was an endo- or exorecycling event, the slope effect of D_2O was determined under activating conditions.

At pH 7.49, pM 7.57, in the presence of NaCl and NaN_3 (100 mM each), ^DV was 2.1 and $^D(V/K_m)_F$ was 1.78 (not shown). From this one could conclude that ∼84% of the D_2O effect on V_{max} came from an endorecycling step. At pH 8.4 the D_2O effect on V/K_m was at least as great as that on V, 2.5-fold, suggesting that all the D_2O effect comes from a rate-determining endo step. A similar D_2O effect on $(V/K_m)_F$ was reported using pig heart enzyme from pM 6.7 to 7.4, in which maximum activation must have been achieved with the 30 mM P_i present (Thomson, 1960). This probably reflects the same endorecycling proton transfer step.

The presence of a slow endo proton transfer is confirmed by a 2-fold D_2O effect on the M/F equilibrium exchange rate with M (32 mM), F (8 mM), and NaCl (100 mM) in 10 mM MOPS, pH 7.0 (not shown). Using up to 100 mM imidazole, in addition to 100 mM NaCl plus 100 mM NaN_3, does not produce any increase in either initial rate or M/F equilibrium exchange (not shown). Presumably the slow endo proton transfer is not accessible to buffer.

Thus, recycling after the F → M conversion requires a rapid proton uptake that may occur after M dissociates from E_m and a second, slow proton dissociation that occurs after F becomes bound to E_{mf}.

DISCUSSION

The F → M conversion rate by fumarase is 4−5-fold activated by simple monoanions at low F concentration when compared with the rate extrapolated to zero ion concentration. Without added anions and at F below activating concentrations, a small but significant basal rate of conversion may remain. Both anions and high substrate increase the M/F equilibrium exchange rate, showing that both influence steps involved in product formation rather than steps of free enzyme interconversion. To simplify matters, the activation caused by substrate is really an anion effect disguised as cooperativity. Thus, malonate activates at concentrations similar to those required for activation by F.

The basis for the large effect of simple salts on the rate of M formation requires further study by structural methods. The low concentration required for many of the salts argues against ionic strength as an explanation. A mechanism based on replacement of charge during product release may be reasonable. It is likely that the carboxylate groups of M will be released in a stepwise manner. For example, in the aconitase reaction the desorption of *cis*-aconitate is slow, allowing the proton abstracted in the dehydration of citrate to appear in the isocitrate product without mixing with free *cis*-aconitate (Rose & O'Connell, 1967). This result and the stereochemistry of the reaction (Gawron et al., 1961) requires the *cis*-aconitate intermediate to undergo major reorientation within the active site without becoming detached, possibly using the carboxymethyl group of this *cis*-aconitate as a pivot point. When the first carboxylate group of M is released in the fumarase reaction, charge neutralization of the exposed positive residue by nonspecific anions would prevent its fall back, accelerating complete release of the product.

The activating effect on M formation due to anions determines the pathway used after liberation of M. This is shown from the influence of NaCl on the inhibition patterns obtained with glycerol (Figure 4). Without anions, glycerol causes a decrease in both V_{max} and $(V/K_m)_F$, indicating that the glycerol-sensitive step either precedes or is coincident with release of M. In the presence of anions that increase product formation there is little change in V/K_m upon addition of glycerol in spite of large effects on V_{max}, suggesting that the step inhibited by glycerol follows the salt-activated M-off step. Thus, the steps responsible for the glycerol effect and

Scheme 2

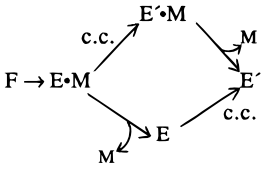

product dissociation would be independent. If that were also true in the unactivated case, the rate-limiting, glycerol-sensitive step must precede and not be coincident with the release step. These alternatives are pictured in Scheme 2, in which the first step of the lower path is activated by anions. The nature of E and E′ will be discussed below. The possibility that the conformational change (c.c.) occurs in recycling implies that its reverse has occurred at an earlier point in the cycle. This primary conformational change must be rapid as there is little effect of glycerol on slope in the presence of NaCl (Figure 4) or on the rate of M/F exchange at equilibrium (data not shown). Its source may be the reaction itself, which would not be detected by either of these kinetic methods due to its great rate relative to endo- events such as product release.

The increase in equilibrium exchange rate by 100 mM NaCl at low (M + F) (Figure 2) seems to offset a second salt effect on recycling (Figures 7 and 8 and Table 1). Thus, in Figure 3, the K_α, which reflects the recycle/exchange ratio of free enzyme, does not increase with increasing NaCl as long as the exchange rate is also increasing. The basis for the activation of recycling could be analyzed only when effects on the concentration of E_m in the steady state could be determined. Observation of noncompetitive inhibition by mesotartarate in the direction F → M indicates that there is a significant amount of E_m (M-specific) that is "slowly" converted to a species with which F can react in the steady state. Factors that increase K_α, such as high Cl^-, N_3^-, phosphonate, and imidazole (Table 1), also decrease E_m as shown by the increased K_{ii} of mesotartarate (Figures 7, 9, and 11). These effects have been interpreted as activation of the recycling of E_m. Alternately, such effects might result from a change in the sequence of steps, as was used to explain the effect of anions in Scheme 2. If these activators favored the release of a nonspecific isoform, E_{mf} instead of E_m, the concentration of E_m would be decreased and K_α would increase. In this case the conformational restructuring would have to become endo. One would expect *V/K* to change as K_{ii} increased, which is not observed with any of these activators (Figures 7, 9, and 11). The practically parallel nature of these double-reciprocal plots also means that any alternate path for M formation must not be significantly influenced by high salt, imidazole, or phosphonate. Therefore the effect of these factors on K_α and K_{ii} reflects an increased recycling of E_m. When made rapid enough by these activators, mesotartarate behaves like a competitive inhibitor, *i.e.*, E_m has been converted to a species with affinity for both F and mesotartarate, and therefore presumably M. This suggests that E_m recycles to a nonspecific species, $E_m \rightarrow E_{mf}$, rather than to an F-specific form with which mesotartarate would not interact (Figure 6).

The interaction of F with E_{mf} must be functional, a part of the cycle and not a dead-end interaction since one never observes inhibition with very high amounts of F. As will be shown in a subsequent report, recycling in the M → F direction results in formation of an F-specific isoform, E_f, which also progresses to a nonspecific form, presumably the same E_{mf}. With F as substrate the $E_{mf} \rightarrow E_f \rightarrow E_f$•F path will be replaced by $E_{mf} \rightarrow E_{mf}$•F $\rightarrow E_f$•F as F increases. Any recycling event that occurs in $E_{mf} \rightarrow E_f$ would have to occur in the interconversion of the F-liganded complexes. Bypassing the $E_{mf} \rightarrow E_f$ conversion as F increases could become the basis for cooperative kinetics when earlier steps are made rapid by the presence of an activator of $E_m \rightarrow E_{mf}$ (Britton, 1997). This possibility was examined at pH 7.4 in the presence of 100 mM NaCl and 100 mM NaN_3. No curvature in the double-reciprocal plot was seen over the range 0.05−4.5 mM F. Thus the K_m of F for reaction with E_{mf} must be quite low, or the transition of E_{mf} to E_f must be very slow.

When do the proton transfers occur in the reaction cycle? The α subsite becomes protonated in the F → M direction by abstraction from the cosubstrate H_2O as part of the rapid chemical conversion. Deprotonation of this site must be the source of the D_2O effect in this direction inasmuch as proton transfers are rapid from the β subsite (no discrimination against T in the formation of M in T-water). Under conditions giving rapid release of M, 100 mM NaCl, with $E_m \rightarrow E_{mf}$ made rapid by P_i, V/K_m shows ∼2-fold D_2O effect. Likewise, a similar D_2O effect on M/F exchange at equilibrium establishes the site of dissociation of the α site as endo. Therefore, the α-proton must recycle either before M dissociates or after F interacts with E_{mf}. Absence of a D_2O effect on K_{ii} of mesotartarate rules out deprotonation of the α site prior to M formation. Thus, the α site, which becomes protonated in the F → M conversion, is only restored when the next cycle has begun. The importance of this step in determing k_{cat} will require knowledge of its intrinsic D_2O effect. As H_2O is known to exchange before F in the M → F direction (Hansen et al., 1969), accessibility of the α site to protons of the solvent at this point in the cycle is assured.

The β site becomes protonated by the M → F reaction and must be deprotonated for the next reaction with M. At what point in the recycling path does this exchange occur? The observation (Rose et al., 1992) that T derived from 3T-malate is captured by F at low concentration (∼0.1 mM) indicates that exchange from the β site of E_{mf} is slow or nil. On the other hand, the absence of T discrimination for M synthesis in T-water requires that the β site is rapidly protonated. Therefore, the β-proton of E_{mf} may exchange with solvent only after a slow step, such as $E_{mf} \rightarrow E_m$. This could explain the observation that capture by F as a fraction of the total T of 3T-malate that is mobilized was decreased as the concentration of M was increased (Rose et al., 1992). This phenomenon has been confirmed with mesotartarate and the yeast enzyme; *i.e.*, added mesotartarate raises the concentration of F required for capture of T derived from 3T-malate (not shown). Thus, exchange of the β-proton occurs from both E_m and E_m•M. It is curious that the two protons that must be lost for recycling to occur in the two directions are not lost until the substrate binds to the otherwise fully recycled enzyme. The site at which the α site is reprotonated in the M → F direction will be considered in a subsequent paper.

Support for early protonation of the β site in the F → M direction comes from the effect of pH on K_{ii} of mesotartarate (Figure 12). E_m interacts with mesotartarate about 6× more tightly at pH 7.4−8.4 than at pH 5.4−6.0. Since the α site is protonated when M is formed, Scheme 1, and since its deprotonation for the next cycle with F occurs at a late step of the cycle, as already discussed, the states of E_m at these

extremes of pH would be $E_{\beta}^{\alpha H}$ and $E_{\beta H}^{\alpha H}$, respectively. The protonation of the β site, preceding the slow $E_m \rightarrow E_{mf}$ transition, is at equilibrium with an apparent pK_a of ~6.7. Protonation of the β site in this pH range probably explains the decrease in $V_{max(M\rightarrow F)}$ that is observed below pH 7.0.

In addition to the solvent as a proton source, imidazolium acts as a general acid (Figure 10) for the β site, as shown by its ability to raise the K_{ii} of mesotartarate (Figure 9) and facilitate recycling of $E_{(m)}^{\alpha H}$ (Table 1). In this mechanism the buffer proton must be transferred in an imidazolium·$E_{\beta(m)}^{\alpha H}$ complex giving imidazole·$E_{\beta H(m)}^{\alpha H}$, which undergoes slow conversion to imidazole·$E_{H(mf)}^{H}$ before dissociation of the imidazole. The absence of a D_2O effect on K_{ii} of mesotartarate supports the conclusion, based on the effect of glycerol, that recycling of E_m is limited by a conformational change, not a proton transfer.

Weaver and Banaszak (1996), using X-ray data for *E. coli* fumarase C complexed with citrate to model in M, have identified H188 acting through an active-site H_2O molecule as the base for abstraction of the methylene H of M. This would be consistent with the pK_a of ~6.7 for recycling of the neutral His residue but requires that T, that is abstracted from 3T-malate, reside on a water that is hydrogen-bonded to His H^+. The high extent of T transfer, exceeding 80% at high F, is more readily explained using the monoprotonic T-carrier that would result with His itself as the abstracting base.

One should consider whether the existence of two enzyme isoforms to which M can bind may have evolutionary significance. Since F cannot bind to E_m, it seems unlikely that the major uneclipsed conformation of M, with the carboxyls anti to each other, would bind either. By this argument the M formed from F would undergo a rapid rearrangement to the more stable, unbindable conformation after and possibly during its release from E_m. Thus, a conformational distortion of the active site would serve the function of improving the desorption of the product. This strategy would not interfere with binding of M in the $M \rightarrow F$ direction inasmuch as nonspecific E_{mf} occurs earlier in the cycle in that direction.

To study the nature of the $E_m \rightarrow E_{mf}$ conformational change requires an analysis of structures that are stabilized in different states. For this a more complete understanding of the specificities of inhibitors will be useful. The conformation of bound mesotartarate might serve to crystallographically distinguish between protein in the E_m and E_{mf} forms, reflecting their different affinities for M and F. In addition, a specific inhibitor for E_f would be useful to identify that form. A greater access to solvent of the β site, probably H188, in E_m than E_{mf} should serve to distinguish these structures in crystals.

Identification of the binding site of P_i, competitive with N_3^- and SCN^-, the most chaotropic anions (Melander & Horvath, 1977; Brzovic et al., 1994) might clarify its role in facilitating $E_m \rightarrow E_{mf}$. Continuing their earlier X-ray analysis of *E. coli* fumarase C, Weaver et al. (1995, 1996) may have identified a possible regulatory site, ~12 Å from the active site, based on binding of a small molecule at the entrance of the pocket in which substrate binds. This region, unlike the substrate binding site, is not conserved in other members of the fumarase superfamily, nor was it essential for activity (Weaver et al., 1997).

The present study should have significance for enzymes other than fumarase. The chemical phase of any enzymatic reaction imposes changes on the enzyme as the enzyme changes the substrate. For some types of reactions, loosely termed rearrangements, reconstruction of the initial active-site configuration may occur in a subsequent half-reaction. For most hydrolases, hydratases, kinases, dehydrogenases, and other transferases, active-site reconstruction must occur after the reaction chemistry. Reconstruction may be slow as indicated by isomechanism kinetics, by counterflow exchange, by D_2O and buffer effects, or by the ability to capture a transferred proton or ^-OH group before dissociation, or reconstruction may be rapid. In either case, processes have been developed in the evolution of the complete enzyme reaction cycle within the constraints of protein structure and the parameters that determine rates of proton transfer that we do not understand in most cases. A dedicated analysis of recycling kinetics combined with structural studies of a variety of enzymes will be required before general principles will become discernible.

REFERENCES

Alberty, R. A., Massey, V., Frieden, C., & Fuhlbrigge, A. R. (1954) *J. Am. Chem. Soc. 76*, 2485−2493.

Anderson, V. E. (1991) in *Enzyme Mechanism from Isotope Effects* (Cook, P. F., Ed.) pp 389−417, CRC Press, Boca Raton, FL.

Berman, K., DiNovo, E. C., & Boyer, P. D. (1971) *Bioorg. Chem. 1*, 234−242.

Britton, H. G. (1973) *Biochemistry 133*, 255−261.

Britton, H. G. (1997) *Biochem. J. 321*, 187−199.

Brzovic, P. S., Choi, W. E., Borchardt, D., Kaarsholm, N. C., & Dunn, M. F. (1994) *Biochemistry 33*, 13057−13069.

Collins, K. D. (1997) *Biophys. J. 72*, 65−76.

Fisher, H. F., Frieden, C., McKinley-McKee, J. S., & Alberty, R. A. (1955) *J. Am. Chem. Soc. 77*, 4436−4440.

Gawron, O., Glaid, A. J., III, & Fondy, T. P. (1961) *J. Am. Chem. Soc. 83*, 3634−3640.

Hansen, J. N., DiNovo, E. C., & Boyer, P. D. (1969) *J. Biol. Chem. 244*, 6270−6279.

Keruchenko, J. S., Keruchenko, I. D., Gladilin, K. L., Zaitsev, V. N., & Chirgadze, N. Y. (1992) *Biochim. Biophys. Acta 1122*, 85−92.

Melander, W., & Horvath, C. (1977) *Arch. Biochem. Biophys. 183*, 200−215.

Porter, D. J. T., & Bright, H. J. (1980) *J. Biol. Chem. 255*, 4772−4780.

Rebholz, K. L., & Northrop, D. B. (1994) *Arch. Biochem. Biophys. 312*, 227−233.

Rebholz, K. L., & Northrop, D. B. (1995) *Methods Enzymol. 249*, 211−240.

Rose, I. A., & O'Connell, E. L. (1967) *J. Biol. Chem. 242*, 1870−1879.

Rose, I. A., O'Connell, E. L., Litwin, S., & Bar Tana, J. (1974) *J. Biol. Chem. 249*, 5163−5168.

Rose, I. A., Warms, J. V. B., & Kuo, D. J. (1992) *Biochemistry 31*, 9993−9999.

Rose, I. A., Warms, J. V. B., & Yuan, R. G. (1993) *Biochemistry 32*, 8504−8511.

Sweet, W. L., & Blanchard, J. S. (1990) *Arch. Biochem. Biophys. 277*, 196−202.

Thomson, J. F. (1960) *Arch. Biochem. Biophys. 90*, 1−6.

Weaver, T. M., & Banaszak, L. V. (1996) *Biochemistry 35*, 13955−13965.

Weaver, T. M., Levitt, D. G., Donnelly, M., Wilkens-Stevens, P., & Banaszak, L. V. (1995) *Nat. Struct. Biol. 2*, 654-662.

Weaver, T. M., Lees, M., & Banaszak, L. (1997) *Protein Sci. 6*, 834−842.

BI971258D